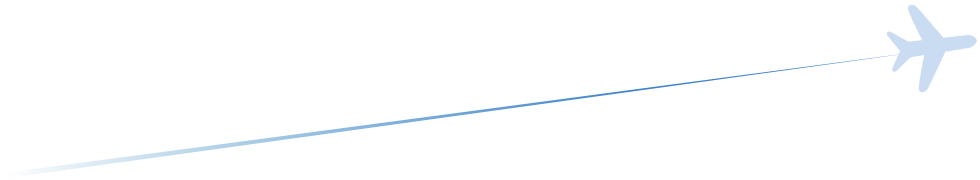

D4.1 Advanced prediction models for flexible trajectory-based operations

Deliverable D4.1

ADAPT

Grant:	**783264**
Call:	**H2020-SESAR-2016-2**
Topic:	**SESAR-ER3-03-2016 Optimised ATM Network Services: TBO**
Consortium coordinator:	**Università degli Studi di Trieste**
Edition date:	**28 February 2019**
Edition:	**01.01.00**

Founding Members

EUROPEAN UNION EUROCONTROL

SESAR JOINT UNDERTAKING

Authoring & Approval

Authors of the document

Name/Beneficiary	Position/Title	Date
Mihaela Mitici /TUD	WP04 Leader/Assistant Professor	25 February 2019
Rene Verbeek/TUD	WP04 Contributor/Senior Researcher	25 February 2019
Remon van den Brandt/TUD	WP04 Contributor/ Researcher	25 February 2019

Reviewers internal to the project

Name/Beneficiary	Position/Title	Date
Tatjana Bolic	Project member/Senior Researcher	26 February 2019

Approved for submission to the SJU By — Representatives of beneficiaries involved in the project

Name/Beneficiary	Position/Title	Date
Lorenzo Castelli	Project Coordinator/Assistant Professor	28 February 2019

Rejected By - Representatives of beneficiaries involved in the project

Name/Beneficiary	Position/Title	Date
N/A		

Document History

Edition	Date	Status	Author	Justification
00.01.00	20 December 2018	Draft	ADAPT Consortium	Initial draft for internal review
01.00.00	21 December 2018	Release to SJU	ADAPT Consortium	New document for review by SJU
01.01.00	28 February 2019	Release to SJU	ADAPT Consortium	Review comments addressed

ADAPT

ADVANCED PREDICTION MODELS FOR FLEXIBLE TRAJECTORY BASED OPERATIONS

This deliverable is part of a project that has received funding from the SESAR Joint Undertaking under grant agreement No 783264 under European Union's Horizon 2020 research and innovation programme.

Abstract

This deliverable summarises the methodological approach to assess and adjust strategic flight planning at the pre-tactical and tactical level by taking into account the inherent uncertainty associated with the operations. The methodology is conducive to the trajectory-based operations. The objective of the methodology is to provide increased flexibility to flights while taking into account network constraints and probabilistic trajectory times. The proposed solution is a stochastic optimization model that assigns time windows to flights. The width of the time windows is a metric for flight flexibility. The results show that using a stochastic approach, more flexibility can be assigned to flights. Next steps are to assess the impact on flight performance of different time window lengths by means of extensive simulation.

Table of Contents

Executive summary

The scope of ADAPT is to propose a set of methods and tools (a solution) at the strategic pre-tactical level of network management that is conducive to the trajectory-based operations. The ADAPT solution provides the trajectory-based operations with flexibility while satisfying the network constraints. This approach relies on the fact that information between all stakeholders is shared at an early stage, up to 6 months in advance from the day of the operations. The same framework for information sharing is maintained also at the pre-tactical and tactical phase.

The ADAPT project creates and tests models and metrics that enable strategic planning (early information sharing), by providing the information on flight flexibility and bottlenecks in the network. Such models are further assessed and adjusted at the pre-tactical and tactical level by taking into account the inherent uncertainty associated with the operations. To address the pre-tactical and tactical level, the ADAPT objective is to identify main sources of uncertainty that could lead to imbalances in the network and to develop models that allow for flight flexibility given stochastic model parameters such as, for instance, flight entry times in a sector.

To allow the assessment and adjustment of strategic models at the pre-tactical and tactical level, a three-step approach is followed: i) identification of main sources of uncertainty associated with trajectory-based operations; ii) development of a set of stochastic models that are able to take into account probabilistic model parameters and adjust flight flexibility, when required. These probabilitistic parameters are necessary to quantify the level of uncertainty of the operations; iii) evaluation and comparison of the strategic and stochastic models by means of a simulation of the operations. The main objective of this last step is to evaluate the magnitude of the potential flight adjustments as a result of uncertainty. Also, the impact of the new solution on the individual flight punctuality and fuel consumption is estimated.

Next steps are to extend the evaluation of the ADAPT solutions, i.e., the time windows associated with each flight, by means of extensive simulations. The aim of the simulations is to assess the impact of the width of the TWs on the flight time and the fuel consumption needed to adhere to the required TWs.

1 Introduction

The scope of ADAPT is to propose a set of methods and tools (a solution) at the strategic pre-tactical level of network management that is conducive to the trajectory-based operations. This solution provides the trajectory-based operations with flexibility while satisfying the network constraints. The ADAPT project creates and tests models and metrics that enable strategic planning (early information sharing), by providing the information on flight flexibility and bottlenecks in the network. This deliverable extends these strategic models at the pre-tactical and tactical level by taking into account the inherent uncertainty associated with the operations.

To allow the assessment and adjustment of strategic models at the pre-tactical and tactical level, a three-step approach is followed:

i) identification of main sources of uncertainty associated with trajectory-based operations. These sources results in probabilistic aircraft trajectory times.

ii) development of a set of stochastic models that are able to take into account probabilistic model parameters and adjust flight flexibility, when required. These probabilitistic parameters are necessary to quantify the level of uncertainty of the operations;

iii) evaluation and comparison of the strategic and stochastic models by means of a simulation of the operations.

The main sources of uncertainty considered in the analysis have been the uncertainty related to weather conditions, and in particular, the wind uncertainty along the trajectories, as well as departure delays. These uncertainties are necessary to determine probabilistic trajectory times.

Further, we have developed a stochastic model that assigns time windows (TWs) to flights taking into account en-route capacity constraints and generic, probabilistic trajectory times. To illustrate our approach, we consider the uncertainty in trajectory times due to weather conditions. Weather ensembles from the European Centre for Medium-Range Weather Forecasts (ECMWF) have been employed to model the uncertainty due to weather conditions. The TW model aims to provide as much flight flexibility as possible in the form of TWs associated with each flight. At the same time, the model ensures that the sector capacity is satisfied.

The evaluation of the strategic and stochastic flight TWs takes as input the flight trajectories (waypoints, aircraft type) available in DDR2 and the TWs obtained from the strategic and stochastic models. The aircraft trajectories are simulated, using the open-source BlueSky simulator. Apart from simulating the aircraft trajectories, BlueSky has embedded functionalities for aircraft performance

modelling using BADA 3 [4]. As such, the fuel consumption and flight time are estimated for a given trajectory, for a given weather ensemble. To evaluate the impact on fuel consumption of the strategic and stochastic TWs, a new aircraft functionality has been added to BlueSky. This functionality can take into account the opening and closing times of the TWs. As a result, given a trajectory and a weather ensemble member, the fuel consumption and the flight time is evaluated for a given type of TW (strategic or stochastic TW model). This analysis allows for comparisons between the performance of the strategic and stochastic TW models with respect to fuel consumption and flight time.

The remainder of this deliverable is organized as follows. In Section 2 we discuss several sources of uncertainty that impact aircraft trajectory times. In Section 3 we propose a stochastic model that adjusts the strategic TWs by taking into account probabilistic aircraft trajectory times. As a demonstration of our approach we consider probabilistic aircraft trajectories due to meteorological uncertainty. In Section 4 we assess the strategic and stochastic TWs by means of simulation. We evaluate the fuel consumption and flight times of the aircraft trajectories when the strategic and the stochastic TWs are required. Finally, in Section 5 the next steps are proposed for expanding the performance analysis of the proposed models using additional simulations

2 Aircraft trajectory timing predictions

In the context of air traffic operations, uncertainty is commonly defined as the condition of being partially or completely in doubt about the precision of certain quantitative values [2]. These can, for example refer to the state of an aircraft (e.g. aircraft velocity or position). How much doubt exists about the precision of these values is typically a function of the look-ahead time. In air traffic operations, the first trajectory predictions have to be made months in advance of the actual flight (e.g., when airlines apply for airport slots). At this phase a lot of uncertainty is present , for example, due to weather conditions. At the pre-tactical and tactical phase, new information such as weather reports allow for better predictions and result in less uncertainty.

Below we discuss 2 main sources of uncertainty i) the uncertainty generated by the meteorological conditions and, in particular, wind and ii) the uncertainty in the departure time. We consider these sources of uncertainties for aircraft trajectories obtained from the Data Demand Repository (DDR2) from EUROCONTROL [7], which provides data on historical flight data within the European airspace.

2.1 Meteorological conditions - Wind forecasts

We consider the European Centre for Medium-Range Weather Forecasts (ECMWF) [3] and in particular, the TIGGE dataset which consists of ensemble forecast data from 10 global Numerical Weather Prediction (NWP) centres [8]. The ensemble forecast consists of 50 different ensemble members. Each member of the forecast is made with a slightly perturbed initial condition. The spread in the ensemble members is used as a measure of the uncertainty present in the weather forecast.

The wind speed V_w is defined in the dataset as a vector in both the Northward and Eastward component as a function of the latitude (ϕ), longitude (λ), time (t), pressure level (p), and the ensemble member number (e).

$$V_w = \begin{bmatrix} V_{w_n}(\phi, \lambda, t, p, e) \\ V_{w_e}(\phi, \lambda, t, p, e) \end{bmatrix} \tag{2.1}$$

The mean wind speed is given by taking the average of the ensemble members.

$$\overline{V}_w(\phi, \lambda, t, p) = \frac{1}{n}\sum_{e=1}^{n} V_w(\phi, \lambda, t, p, e) \tag{2.2}$$

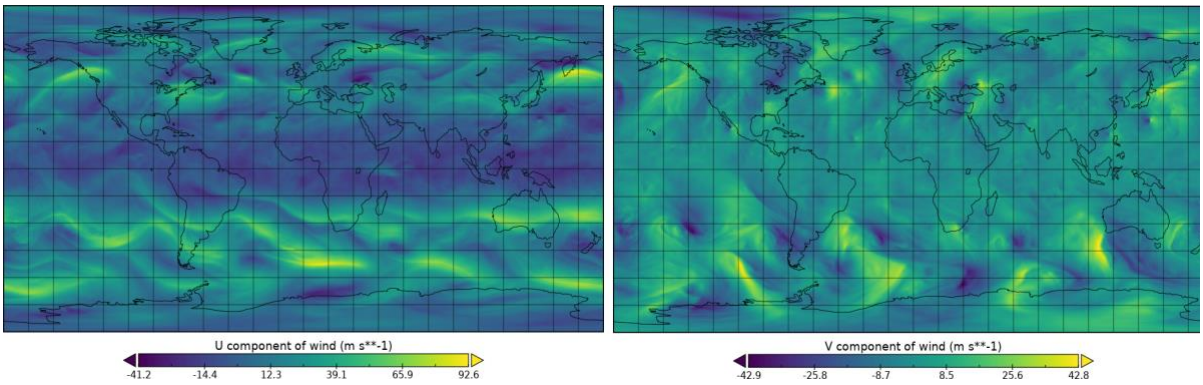

Figure 1. Example of a wind field from the Tigge dataset on the 1st of September 2017.

Furthermore, the magnitude is given as the length of the wind vector

$$|V_w(\phi, \lambda, t, p, e)| = \sqrt{V_{w_n}(\phi, \lambda, t, p, e)^2 + V_{w_e}(\phi, \lambda, t, p, e)^2} \tag{2.3}$$

Figure 1 shows an example of the Northward and Eastward component of the wind field from the Tigge dataset at the 1st of September 2017. Apart from varying per location, pressure level and time, each ensemble member is slightly different because of the perturbed initial conditions.

Figure 2 shows that for a large forecasting time horizon, the variance in the wind forecast is large, thus making it harder to predict the trajectory of an aircraft. As the time of execution becomes closer, the forecast models provide a more accurate estimation of the along track wind. At the 12 h lead time, only a small amount of variance is left between the ensemble members.

The DDR2 database provides both waypoints and the time of crossing a waypoint. From this, we compute the ground speed (V_g) of the aircraft, assuming that it stays constant in between each set of waypoints. From the ground speed, V_{TAS} can be calculated by subtracting the wind speed (2.4), after which the new wind speed can be substituted to calculate the updated ground speed under influence of a weather ensemble.
The new ground speed can be obtained by solving a quadratic equation.

$$V_{TAS} = \sqrt{(V_g \cos\psi - V_{w_n})^2 + (V_g \sin\psi - V_{w_e})^2} \tag{2.4}$$

where V_{w_n} and V_{w_e} are the Northward and Eastward components of the wind respectively, and ψ is the aircraft course. In practice, flights operate using the ECON mode of their FMS [11]. ECON climb, cruise, and descent speeds are based on the Cost Index (Cost of Time/Cost of Fuel). The airlines can decide, however, to change the Cost Index, and thus, to specify a new ECON mode when this is beneficial for the airline either from a flight time perspective or from a fuel cost perspective. In particular, ECON mode may be set such that the VTAS is adjusted for unfavourable wind conditions. Thus, changes in VTAS can be achieved by making use of different cost indices.

After expansion and collection of the terms in eq. (2.4)

$$V_g^2(\cos^2\psi + \sin^2\psi) - V_g(2\cos\psi V_{w_n} + 2\sin\psi V_{w_e}) + V_{w_n}^2 + V_{w_e}^2 - V_{TAS}^2 = 0 \qquad (2.5)$$

the equation can be solved for V_g.

2.2 Departure delay

According to the Central Office for Delay Analysis (CODA) [5], [6], the average departure delay in 2017 was 12.4 min making it one of the largest contributors to flight delay.

Figure 3 shows the distribution of the flight departure delay at all European airports in September 2017. The flight departure delay is determined by comparing the planned flight departure time (M1 files) with the actual

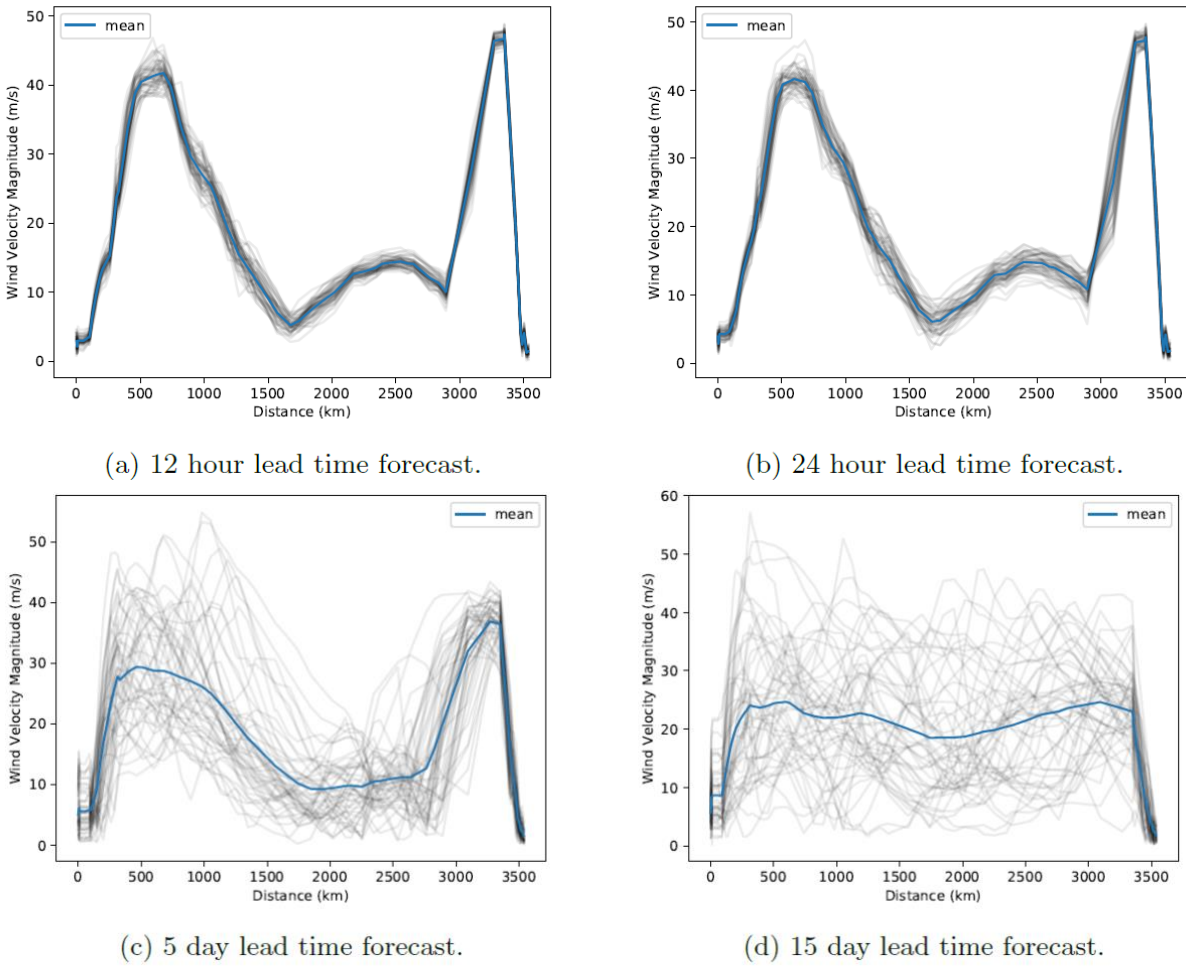

(a) 12 hour lead time forecast.

(b) 24 hour lead time forecast.

(c) 5 day lead time forecast.

(d) 15 day lead time forecast.

Figure 2 Wind velocity magnitude along track of an example trajectory from OLBA to EGLL, the blue line represents the mean of the set and the gray lines represent the individual ensemble members.

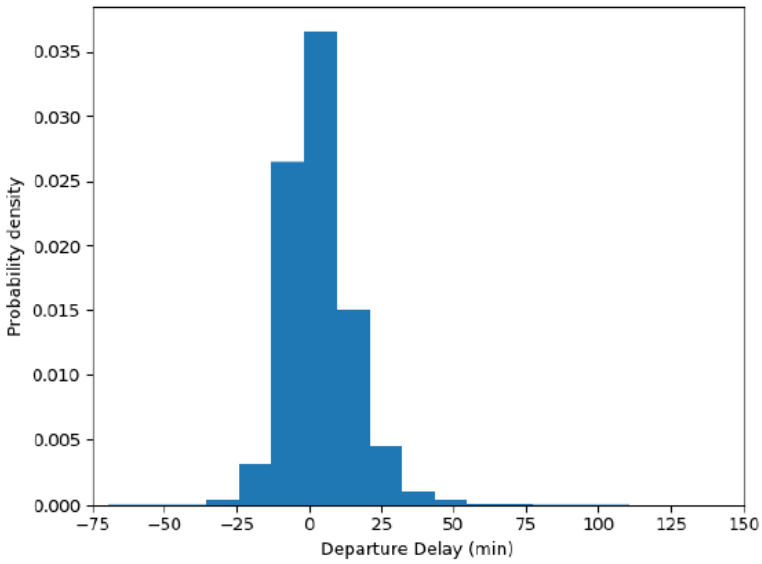

Figure 3 Distribution of Departure Delay

flight departure times (M3 files), which are available in DDR2. Figure 3 shows that the departure delay is concentrated between (-5 min, +15 min) around the planned departure time, while departure delays larger than 25 min are less probable.

In the next section, we will take into account the uncertainty associated with wind speeds and departure delay in the analysis of flight flexibility.

2.3 Other sources of uncertainty

Several other sources of uncertainty may affect the aircraft arrival punctuality in a sector such as, for intance, aircraft performance related uncertainty [10] initial consitions of the aircraft state variables at departure, aircraft motion modeling, differences between actual and modelled gravitational force. Also, ATM-related unplanned events such as reconfiguration of the sectors along aircraft trajectories, change of cruise altitude and airport departure procedures, e.g., SID selection, may also generated unforsee deviations from the flight plans. However, events such as changes in SID selection are much more difficult to predict at the pre-tactical level. In this study we restrict ourselves to analyzing weather related uncertainties, where reliable forecasts are available several days to hours before the flight execution day and departure delay uncertainties as they are expected to induce significant deviations from the flight plans. However, our model is general and can accommodate any type of arrival time distributions. Having obtained probability distributions for the deviations from the planned trajectories due to other sources of uncertainty (aircraft performance, ATM events), our model has the ability to account for these probabilities in the TW optimisation model. Depending on the magnitude of the uncertainty of other sources on a specific flight leg, the TWs will be adjusted according to the model we propose in the next section.

3 Stochastic TW optimisation for aircraft trajectories

At the strategic level, individual flights are assigned TWs in Work Package 3 (WP 3). These are characterized by their opening and closing times. However, uncertainties may impact aircraft trajectory times. In this section we consider probabilistic trajectory times such as, for instance, probabilistic sector entry times associated with trajectories. The model accommodates a generic probabilistic distribution of trajectory times. As an illustration of the model, probabilistic trajectory times due to uncertainty in meteorological conditions, e.g., wind uncertainty, are assumed. The stochastic TW model extends the strategic TW model by implementing stochastic constraints with respect to sector capacity. The output of the stochastic TW model is an updated set of TWs, as compared to the strategic TWs, which takes into account uncertainty.

Section 3.1 gives the strategic TW model as developed in WP3. The extension of this model, to include stochastic constraints and probabilistic trajectory times, is given Section 3.2. We further propose a bi-directional expansion of the strategic TWs, also taking into account probabilistic trajectory times. Finally, the outcome of the strategic and stochastic models are compared in Section 3.3.

3.1 Strategic TWs model developed in WP03

In WP03, a strategic, deterministic TW model is developed , which provides TWs for each flight. These TWs have an opening time and a closing time. The length of the time windows is a measure of flexibility. The time windows are setup in a way that the capacity constraints on the sectors and airports are not violated as long as an aircraft stays within its TW [1]. For completeness, in this section we introduce the strategic TW model developed in WP03.

3.1.1 Notation

For the optimization model, the following notation will be used:

$$\begin{aligned} \mathcal{A} &\equiv \text{set of airports, indexed by a} \\ \mathcal{S} &\equiv \text{set of sectors, indexed by s} \\ \mathcal{F} &\equiv \text{set of flights, indexed by f} \\ \text{orig}_{\text{f}} &\equiv \text{airport of departure of flight f} \end{aligned}$$

$\text{dest}_f \equiv$ airport of arrival of flight f
$\mathcal{R} \equiv$ set of routes, indexed by r, with r_f the chosen route for flight f
$n_f \equiv$ the number of elements (sectors and airports) along the chosen route r_f
$s_r^i \equiv$ i-th sector of route r
$l_r^i \equiv$ flight time from origin to the i-th sector of route s_r^i
$d_f \equiv$ scheduled departure time for flight f
$w_{min} \equiv$ minimum width of each time window
$w_{max} \equiv$ maximum width of each time window
$\mathcal{T}_f^i \equiv \{d_f + l_{r_f}^i, \dots, d_f + l_{r_f}^i + w_{max} - 1\}$
$\equiv$ set of feasible time periods for flight f to arrive at i-th element of its route
$\mathcal{T}^c \equiv \{open_c, \cdots, close_c - 1\}$
$\equiv$ set of time periods during which capacity c is active
$\mathcal{C}_j \equiv$ set of capacity-periods at sector or airport j, indexed by
$open_c \equiv$ opening time period for capacity activation c (i.e. opening time of sector c)
$close_c \equiv$ closure time period for capacity activation c
$\mathcal{C}^c \equiv \{open_c, \dots, close_c - 1\}$
$\equiv$ set of time periods during which capacity c is active
$\mathcal{Q}_c \equiv$ capacity limit enforced during capacity activation c

3.1.2 Decision variables

The TW is defined as a decision variable for each flight f and time period t

$$x_f(t) = \begin{cases} 1, & \text{if TW for flight f is still open for departure at time t} \\ 0, & \text{otherwise} \end{cases} \quad (3.1)$$

$x_f(t)$ is a binary, monotone decreasing variable

$$x_f(t) \geq x_f(t+1) \quad \forall f \in \mathcal{F}, t \in \mathcal{T}_f^0 \quad (3.2)$$
$$x_f(t) \in \{0,1\} \quad \forall f \in \mathcal{F}, t \in \mathcal{T}_f^0 \quad (3.3)$$

where constraint (3.2) enforces that the time window is monotone decreasing and equation (3.3) ensures that the variable is binary. An example TW is given in Table 1. If $w_f(t)$ is equal to one at time t the TW is opened. In this example the TW is opened from $t = 1$ up and until $t = 3$.

Table 1 Example strategic time window for a single flight

t	1	2	3	4	5
$w_f(t)$	1	1	1	0	0

3.1.3 Objective Function

To provide the maximum amount of flexibility, the objective of the optimization algorithm is to maximize the length of the TWs, while adhering to the declared capacity. However, this could lead to an unfair distribution of the available capacity. A fairness measure is implemented in Equation (3.5). This measure favours two medium-length TWs over one long-length TW and one short-length TW in order to prevent unfair assignments of the time windows.

The value functions is given as

$$\max \sum_{f \in F, t \in \mathcal{T}_f^0} x_f(t) \cdot \gamma(t - d_f) \tag{3.4}$$

where the cost coefficient γ is expressed as

$$\gamma(\tau) = 1 - \frac{\tau}{w_{max} \cdot |\mathcal{F}|} \quad 0 \leq \tau \leq w_{max} - 1 \tag{3.5}$$

with $\mathbf{d_f}$ being the scheduled departure time of flight $\mathbf{f}$. The maximum size of the time window $\boldsymbol{\tau}$ is $\mathbf{w_{max}}$.

3.1.4 TW Constraints

Apart from the constraints set in Equations (3.2, 3.3) additional constraints are needed to ensure that the solution does not exceed the declared capacity. First, Equation (3.6) ensures that each flight is assigned a TW of at least one minute. Next to a minimum width of the TW, Equation (3.7) will enforce a maximum length of the TW, by defining $\mathcal{T}_f^i$ to contain exactly a number of time periods equal to w_{max}.

$$x_f(d_f + w_{min} - 1) = 1 \quad \forall f \in \mathcal{F} \tag{3.6}$$

$$\mathcal{T}_f^i = \{d_f + l_{r_f}^i, \dots, d_f + i_{r_f}^i + w_{max} - 1\} \tag{3.7}$$

3.1.5 Capacity Constraints

The second set of constraints will ensure that the declared capacity is respected, (e.g. the amount of flights entering within a given period cannot exceed the capacity). Four different types of capacities are considered; arrival capacity, departure capacity, capacity (total airport movements), and the sector capacity.

$$\sum_{\substack{f\in\mathcal{F},t\in\mathcal{T}^c:\\ dest_f=k\wedge v_{f,t}^{n_f-1}(c)}} x_f(t) \le \mathcal{Q}_c \quad \forall k\in\mathcal{K}, c\in\mathcal{C}_k^{arr} \tag{3.8}$$

$$\sum_{\substack{f\in\mathcal{F},t\in\mathcal{T}^c:\\ orig_f=k\wedge v_{f,t}^{0}(t)}} x_f(t) \le \mathcal{Q}_c \quad \forall k\in\mathcal{K}, c\in\mathcal{C}_k^{dep} \tag{3.9}$$

$$\sum_{\substack{f\in\mathcal{F},t\in\mathcal{T}^c:\\ orig_f=k\wedge v_{f,t}^{0}(c)}} x_f(t) + \sum_{\substack{f\in\mathcal{F},t\in\mathcal{T}^c:\\ dest_f=k\wedge v_{f,t}^{n_f-1}(c)}} x_f(t-l_{r_f}^{n_f-1}) \le \mathcal{Q}_c \quad \forall k\in\mathcal{K}, c\in\mathcal{C}_k^{gen} \tag{3.10}$$

$$\sum_{\substack{f\in\mathcal{F},i\in[1,n_f-1],t\in\mathcal{T}^c:\\ s_{r_f}^{i}=j\wedge v_{f,t}^{i}(c)}} x_f(t-l_{r_f}^{i}) \le \mathcal{Q}_c \quad \forall j\in\mathcal{S}, c\in\mathcal{C}_j^{ent} \tag{3.11}$$

where

$$v_{f,t}^{i}(c) = (\nexists x_f(t-l_{r_f}^{i}-1)) \vee (t-l_{r_f}^{i}-1\notin\mathcal{T}^c) \tag{3.12}$$

$v_{f,t}^{i}(c)$ determines whether time period t is the first period when flight f may reserve capacity for capacity activation c.

3.2 Stochastic TW Model

In this section we extend the strategic, deterministic model with TWs from WP03 (Section 3.1) by considering probabilistic trajectory times. The stochastic TW model assumes a generic probability distribution of trajectory times. To illustrate our approach we consider probabilistic trajectory times due to meteorological uncertainties, in particular, wind uncertainties.

The weather ensembles that capture wind uncertainties, as presented in Section 2, are used as an input to the stochastic model. The probabilistic sector entry time of a flight is then determined using the variation of the wind speed described in each of the 50 weather ensemble members. Taking into account the spread of the wind speed V_w^*, the probabilistic ground speed over a track leg i is computed by Equation (3.16), where Distance(i-1, i) is the length of track leg betwen waypoints i-1 and i, and $\mathrm{Time}(i-1,i)$ is the associated flight time on the leg.

$$V_w^*(\phi,\lambda,t,p,e) = V_w(\phi,\lambda,t,p,e) - \overline{V}_w(\phi,\lambda,t,p) \tag{3.13}$$

$$V_g = \text{Distance}(i-1,i)/\text{Time}(i-1,i) \tag{3.14}$$

$$V_g^* = V_g + V_w^* \tag{3.15}$$

$$t^* = \frac{\text{Distance}(i-1,i)}{V_g^*} \tag{3.16}$$

The arrival time at a sector i is influenced by a random process of the underling weather forecast. In our example, each of the ensemble members will result in a different sector entry time S_T:

$$S_T = \{t^1,\cdots,t^{50}\} \tag{3.17}$$

$$= \left\{\frac{\text{Distance}(i-1,i)}{V_g^1},\cdots,\frac{\text{Distance}(i-1,i)}{V_g^{50}}\right\} \tag{3.18}$$

Every discrete random variable T has associated with it a Probability Mass Function (PMF) $f_T: S_T \rightarrow [0,1]$ defined by

$$f_T(t) = P(T=t), \quad t \in \mathcal{S}_T, \tag{3.19}$$

where f_T describes the probability of flight f arriving at sector i at some time t.

3.2.1 Constraints

In order to limit the probability of exceeding the sector capacity, the deterministic capacity constraint Equation (3.11) from the deterministic, strategic TW model (WP03 and Section 3.1) is replaced by the stochastic constraint:

$$P\left(\sum_{\substack{f\in\mathcal{F},i\in[1,n_f-1],\\ t\in\mathcal{T}^c:s_{r_f}^i=j\wedge v_{f,t}^i(c)}} x_f(t-l_{r_f}^i) > \mathcal{Q}_c\right) \leq \xi \quad \forall j\in\mathcal{S}, c\in\mathcal{C}_j^{ent} \tag{3.20}$$

Figure 4 provides an example of the application of this constraint for 2 aircraft. Both y-axis show the arrival time probability of aircraft 1, ac_1, and aircraft 2, ac_2, respectively, for a given sector. For a certain capacity period (in this example from $t=1$ till $t=2$) the probability is equal to the area under the curve, the blue and the green shaded area. In this example, the probability that ac_1 enters the sector in the capacity period from $t=1$ till $t=2$ is equal to 47.73% (e.g. almost half of the total area under the Probability Density Function (PDF) curve is located in the domain $[1,2)$ while ac_2 only has a probability of 2.23% of entering the sector in this capacity period.

Next, the event of an aircraft f entering a sector in a capacity period c is now modelled as a binomial process, with

$$X_f^c = \begin{cases} 1, & \text{with probability p} \\ 0, & \text{with probability } 1-p \end{cases} \tag{3.21}$$

where X_f^c is equal to one with probability p and zero with probability $1-p$ (e.g. flight f is present in capacity period c with probability p). The probability p is determined by integrating the area under the PMF from the sector opening time to the sector closing time.

$$p_f^c = \int_{t^c_{open}}^{t^c_{close}} f_T^f(t)dt \tag{3.22}$$

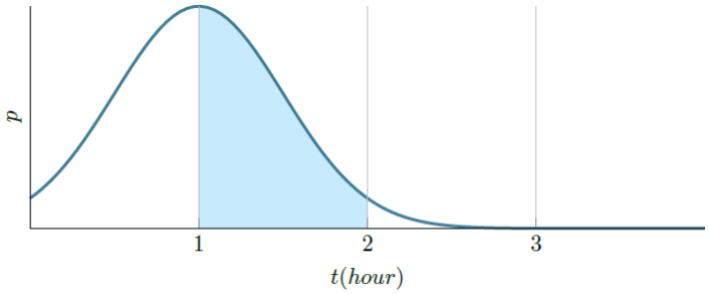

(a) Example probability at a sector in capacity period c for ac_1.

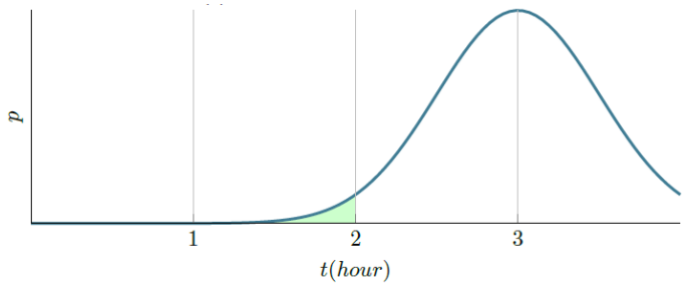

(b) Example probability at a sector in capacity period ac_2.

Figure 4 Illustration of the stochastic capacity constraint for the capacity period $t = 1$ untill $t = 2$.

To apply the stochastic constraint (3.20), we determine the probability that the total number of aircraft present in a capacity period c that exceeds a pre-defined threshold. The total number of aircraft present in a capacity period c is given by:

$$X^c = \sum_{f=1}^{N_{ac}} X_f^c \tag{3.23}$$

The resulting process $\{X^c\}$ is the summation of N_{ac} binomial processes, where N_{ac} is the number of considered aircraft. The resulting process can be approximated by a Poisson binomial distribution with the following properties:

$$X^c \sim \mathcal{N}(\mu_c, \sigma_c^2) \tag{3.24}$$

$$\mu_c = \sum_{j \in \mathcal{S}} p_f^c(t) \cdot x_f(t) \tag{3.25}$$

$$\sigma_c^2 = \sum (1 - p_f^i(t)) p_f^i(t) \cdot x_f(t) \tag{3.26}$$

In the example case of Figure 4, the process describing the amount of aircraft present in the sector between $t = 1$ and $t = 2$ is equal to a normal process with mean $0.4773x_1 + 0.00223x_2$ and a variance of $(1 - 0.4773) \cdot 0.4773x_1 + (1 - 0.00223) \cdot 0.00223x_2$ where x_1 and x_2 are the decision variables that determine if the flights are assigned to the capacity period.

By limiting the area under the PDF of process $\mathcal{N}(\mu_{s,c}, \sigma_{s,c}^2)$ that is greater than the capacity, the probability of exceeding a declared capacity is constrained.

Figure 5 shows how this constraint is implemented. The blue shaded area represents the probability of exceeding the capacity Q_c. When expressed in terms of their standard deviation, the area under the curve is independent of the value of the standard deviation (e.g. $(\mu - \sigma \leq X \leq \mu + \sigma) \approx 0.68$ no matter the value of μ and σ).

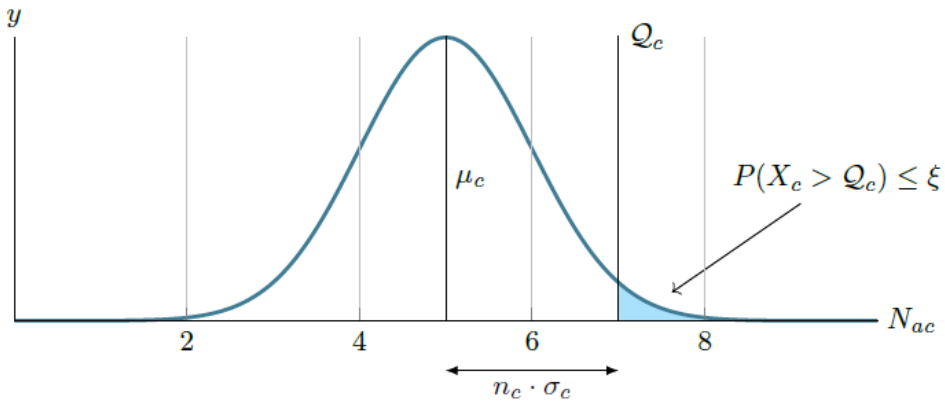

Figure 5 The shaded are under the PDF of process $\mathcal{N}(\mu_c, \sigma_c^2)$ is equal to the probability that the number of aircraft present will exceed Q_c

The probability of exceeding the capacity is

$$P(X_c > \mathcal{Q}_c) \leq \xi \tag{3.27}$$

which can be rewritten as

$$1 - F_c(\mathcal{Q}_c) \leq \xi \tag{3.28}$$

Substituting $\mathcal{Q}_c = \mu_c + n_c \cdot \sigma_c$ into Equation (3.28)

$$1 - F_c(\mu_c + n_c \cdot \sigma_c) \leq \xi \tag{3.29}$$

with the Cumulative Density Function (CDF) ($F_c(x)$) equal to

$$F_c(x) = \Phi\left(\frac{x - \mu_c}{\sigma_c}\right) = \frac{1}{2}\left[1 + \text{erf}\left(\frac{x - \mu_c}{\sigma_c\sqrt{2}}\right)\right] \tag{3.30}$$

where erf is the Gauss error function.

n can be computed by taking the inverse erf function

$$1 - \Phi\left(\frac{\mu_c + n_c \cdot \sigma_c - \mu}{\sigma_c}\right) \leq \xi \tag{3.31}$$

$$1 - \Phi(n_c) \leq \xi \tag{3.32}$$

$$n_c \leq \Phi^{-1}(1 - \xi) \tag{3.33}$$

Now that the value of n is known, the final constraint can be implemented as

$$\mu_c + n_c\sqrt{\sigma_c^2} \leq \mathcal{Q}_c \quad \forall j \in \mathcal{S}, c \in \mathcal{C}_j \tag{3.34}$$

However, since only the standard deviation is available from Equation (3.26), a linear approximation is required. To approximate the square root function, a first order linear approximation will be made by linearizing the function around some point σ_0^2:

$$\sigma_c \approx f(\sigma_0^2) + f'(\sigma_0^2) \cdot (\sigma_c^2 - \sigma_0^2) \tag{3.35}$$

$$\approx \sqrt{\sigma_0^2} + \frac{1}{2\sqrt{\sigma_0^2}}(\sigma_c^2 - \sigma_0^2) \tag{3.36}$$

Finally, constraint (3.20) is implemented as:

$$\sum_{\substack{f\in\mathcal{F}, i\in[1,n_f-1],\\ t\in\mathcal{T}^c: s^i_{r_f}=j \wedge v^i_{f,t}(c)}} \mu_c + n_c\left(\sqrt{\sigma_0^2} + \frac{1}{2\sqrt{\sigma_0^2}}(\sigma_c^2 - \sigma_0^2)\right) \leq \mathcal{Q}_c \quad \forall j \in \mathcal{S}, c \in \mathcal{C}_j^{ent} \tag{3.37}$$

3.3 Extended Stochastic TW Model

The stochastic TW model as developed in Section 3.2 can only be expanded in the positive direction (e.g. a time window can only range from the nominal sector entry time plus a maximum, positive time). This approach limits the flexibility that a flight can have. For example, if a flight is early, due to favorable winds, it cannot enter the sector and has to slow down.

To address this, the TW length in the probabilistic method is extended:

$$\mathcal{T}_f^i = \left\{d_f + l^i_{r_f} - w^-_{max}, \dots, d_f + l^i_{r_f}, \dots, d_f + l^i_{r_f} + w^+_{max} - 1\right\} \tag{3.38}$$

Furthermore, the monotone constraint in Equation (3.2) is modified as follows. The part of the TW from w^-_{max} to 0 will be monotone decreasing while the part beyond 0 to w^+_{max} will be monotone increasing.

$$x_f(t) \geq x_f(t-1) \quad \forall f \in \mathcal{F}, t \in \mathcal{T}_f^0 : t < 0 \tag{3.39}$$

$$x_f(t) \geq x_f(t+1) \quad \forall f \in \mathcal{F}, t \in \mathcal{T}_f^0 : t >= 0 \tag{3.40}$$

An example of the two sided time window is shown in Table 2.

Table 2 Example of an extended TW for a single flight which expands from the nominal sector entry time in both directions.

t	-3	-2	-1	0	1	2	3	4	5
$x_f(t)$	0	0	1	1	1	1	1	0	0

3.4 Results

In this section we compare the results of the deterministic, stategic TW model with the solution obtained from the stochastic TWs model.

The input to the stochastic TW model is identical to the deterministic, stategic TW model, with the exception of the fact that the stochastic TW model requires probabilistic trajectory times. The probabilistic trajectory times are determined using the uncertainty in the weather ensembles, as described in Section 3.2.

By comparing the results of the deterministic solution to the results of the stochastic solution, it is possible to study the effect of the new stochastic constraint. A higher percentage of large TWs will lead to more flexibility in the air traffic management. At the same time, larger TWs will lead to less critical flights (e.g. flights that have a very constraining TWs). In turn, less effort is required to adhere to these TWs, which leads to lower fuel consumption.

Figure 6(a) shows the histograms of the TW length for the strategic TW model (WP03). Figure 6(b) shows the histograms of the TW length for the stochastic TW model. Note that the y-axis is truncated to improve readability, while the total number of flights and their distribution is given in Table 3. The TW length is applied for the entire trajectory of the aircarft. Moreover, the maximum length of the TW is set to 15 min, i.e., the flights are expected to adhere to a TW where the opening time is the optimal entry time in a sector and the maximum closing time is the optimal entry time plus 15 min.

When comparing the solutions of the deterministic, strategic and stochastic TW model it can be seen that the number of TWs with a small length has decreased significantly. Table 3 also shows the change in TWs when comparing the strategic and stochastic TW models. All entries above the diagonal are TWs that increased in size. TWs that remain the same in both solutions are shown on the diagonal. Finally, the entries below the diagonal show the time windows that have shrunk in the stochastic solution. Not only did the amount of small time windows decrease in the absolute sense, there is also a very limited set of time windows which shrunk in the stochastic model, i.e., ($\frac{202}{29535}$ or 0.7%).

Figure 6(c) and Figure 6(d) show the histogram of the negative and positive part of the TW respectively, for the stochastic, two-sided TWs model, as developed in Section 3.3. From this histogram it can be seen that the positive side of the two-sided solution does not change drastically. However, since the TW is also allowed to expand in the negative direction, the total length of the TWs is greater. Furthermore, from Figure 3(c) it can be seen that some flight are constraint from expanding in the negative direction. However, the majority of the flight can increase the time window, thus providing a greater amount of flexibility.

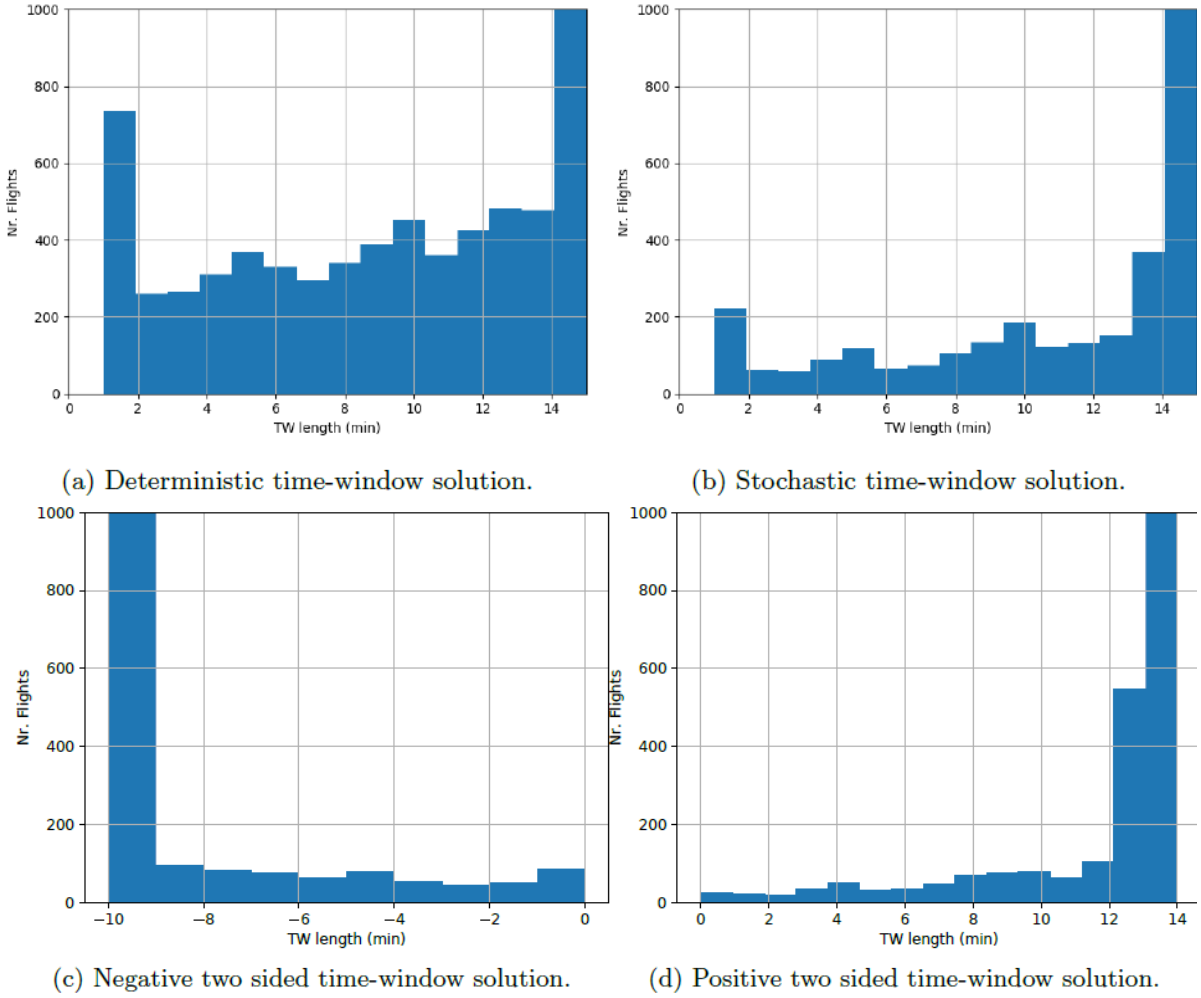

Figure 6 Histogram showing the variation in assigned time windows for both the solutions of the deterministic and the stochastic TW model. On the x-axis the TW length is indicated. On the y-axis the number of flights that have been assigned a specific TW length, is indicated.

Table 3 Number of flights for each TW in the stochastic TW model (y-axis) and the deterministic TW model (x-axis).

Probabilistic TW Length	Deterministic 1	2	3	4	5	6	7	8	9	10	11	12	13	14	15	Total
1	219	0	0	0	0	0	0	0	0	0	0	0	0	0	2	221
2	1	58	1	0	0	0	0	0	0	0	0	0	0	0	2	62
3	1	1	51	0	0	0	0	0	0	0	0	0	0	0	6	59
4	2	1	0	76	0	0	0	0	0	0	0	0	0	0	10	89
5	1	3	1	1	106	0	0	0	0	0	0	0	0	0	7	119
6	0	2	2	1	0	56	0	0	0	0	0	0	0	0	6	67
7	1	0	2	2	3	1	57	0	0	0	0	0	0	0	8	74
8	6	0	0	2	0	3	0	90	0	0	0	0	0	0	6	107
9	5	3	1	0	1	2	2	2	107	0	0	0	0	0	11	134
10	10	3	3	3	0	1	2	1	3	145	0	0	0	0	16	187
11	11	2	1	0	1	0	1	0	1	3	94	1	0	0	6	21
12	6	4	1	4	2	1	0	1	1	2	0	100	0	1	9	132
13	5	0	2	1	1	2	2	2	3	3	0	0	124	0	7	152
14	36	5	5	2	9	4	4	6	7	4	1	3	4	135	104	329
15	433	178	197	219	246	261	229	240	266	295	265	322	355	342	23834	27682
Total	737	260	267	311	369	331	297	342	388	452	360	426	483	478	24034	29535

Table 4 shows in detail the number of aircraft that have been assigned a specific TW length, when allowing for the TW to expand in both directions. In particular, we this TW length is applied for the entire trajectory of the aircarft. The TW are expanded in both around the optimal entry time in a sector, with of (-10 min, +15 min) from this optimal entry time in a sector. Table 4 shows that, compared with the deterministic TW model solution, allowing TWs to expand in both directions leads to a large number of flights having assigned an expansion of the TWs to -10 min from the optimal entry time in a sector. As such, the majority of the flights have assigned a TW with a 25 min length, i.e., (-10min, +15 min).

Table 4 Number of flights for each TW in the stochastic TW model (y-axis) and the deterministic TW model (x-axis).

Probabilistic TW Length	Deterministic 1	2	3	4	5	6	7	8	9	10	11	12	13	14	15	Total
-10	714	253	259	296	359	321	283	331	377	444	352	412	461	467	23565	28894
-9	3	0	2	2	5	2	5	2	1	0	1	2	2	1	67	95
-8	2	3	3	0	1	2	2	3	0	2	1	2	0	1	61	83
-7	3	1	1	1	0	1	1	0	5	2	0	1	3	2	55	76
-6	3	0	1	2	1	2	0	2	2	2	2	3	2	1	43	66
-5	5	1	0	2	0	0	1	0	1	0	0	1	6	3	62	82
-4	0	0	1	2	2	0	0	1	0	0	2	1	2	0	45	56
-3	1	0	0	1	0	1	3	1	1	1	1	0	3	0	31	44
-2	2	0	0	4	0	1	0	0	0	0	0	2	2	1	39	51
-1	2	1	0	0	0	0	1	0	1	1	0	0	2	0	24	32
0	2	1	0	1	1	1	1	2	0	0	1	2	0	2	42	56
1	24	0	0	0	0	0	0	0	0	0	0	0	0	0	1	25
2	1	18	1	0	0	0	0	0	0	0	0	0	0	0	2	22
3	0	1	14	0	2	0	0	0	0	0	0	0	0	0	3	20
4	2	0	0	24	0	0	0	0	0	0	0	0	2	0	8	36
5	1	0	1	0	41	1	0	0	0	0	0	0	0	0	7	51
6	2	0	2	0	0	14	1	0	0	0	0	0	0	0	13	32
7	1	0	0	0	1	0	25	0	0	0	0	0	0	0	8	35
8	3	0	0	1	0	1	0	33	3	0	0	0	0	0	8	49
9	5	3	1	0	1	2	0	0	41	2	0	0	1	0	14	70
10	4	1	2	1	1	2	0	1	1	34	1	0	0	1	28	77
11	2	1	0	0	0	1	2	2	1	1	40	2	2	0	26	80
12	0	2	1	1	0	0	1	1	3	2	2	28	0	1	21	63
13	4	0	1	3	1	1	0	2	1	0	0	1	51	1	39	105
14	55	16	23	11	12	18	12	15	12	9	7	10	10	33	306	549
15	633	218	221	270	310	291	256	288	326	404	310	385	417	442	23550	28321

Departure Delay Analysis

In order to evaluate the TWs in the presence of departure delay, an analysis is performed to see how much of the departure delay distribution is covered by the TW. By calculating the area under the departure delay PDF between the TW opening and closing time, it is possible to estimate the probability of departing within the assigned TW. in Figure 7 gives an example of this process.

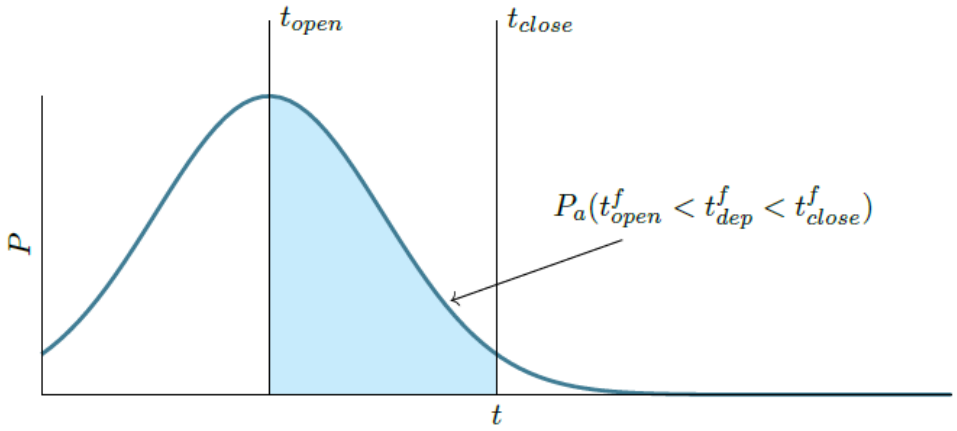

Figure 7 Departure Delay Probability at airport a and flight f

We evaluate the resulting TWs from the strategic and stochastic model against the distribution of the departure delay in September 2017 at the European airports. We determine the distribution of departure delay, given in Figure 8, from DDR2 data by comparing the planned departure time (M1 files) and the actual departure times (M3) files.

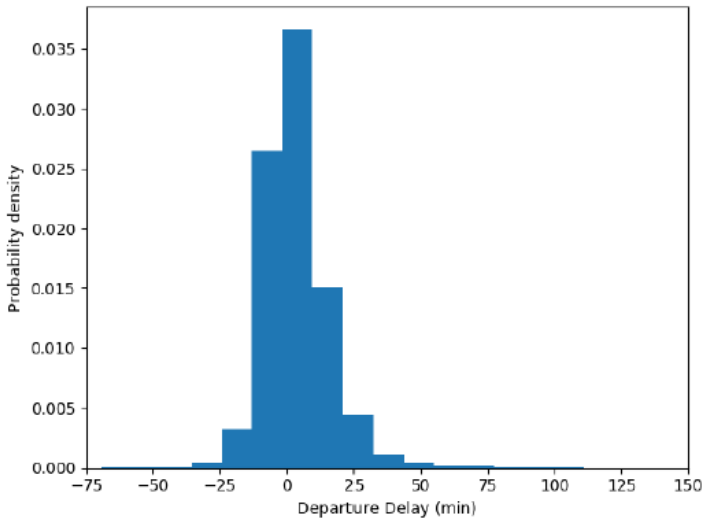

Figure 8 Distribution of departure delay

Table 5 shows the results of the evaluation of $P_a\left(T^f_{open} < t^f_{dep} < T^f_{close}\right)$.

Table 5 shows that for the deterministic TW solution, around 42% of all flights would depart within their assigned TW, given the historical departure delay statistic. For the stochastic TW solution, 44% of all flights depart within their TW. This small difference is expected since the majority of flight have a TW assigned of 15 minutes, both in the deterministic and stochastic TW solution. Finally, in the two-sided stochastic TW solution, 74% of all flights depart within their assigned TW. This effect is mainly caused by the increase in the total time window length.

Table 5 Departure delay adherence

Solution	$P_a\left(T^f_{open} < t^f_{dep} < T^f_{close}\right)$
Deterministic	0.42
Probabilistic	0.44
Two sided	0.74

4 Control model to adhere to TWs using speed adjustments

The TWs developed in Section 3 provide flight flexibility. However, current aircraft are not equipped to take advantage of this added flexibility, using a Requested Time of Arrival (RTA). A new FMS algorithm that supports the usage of TWs is introduced in this section after a generic description of the conventional FMS in Section 4.1. Next, the performance of the TWs in combination with the new FMS will be evaluated in terms of fuel consumption and punctuality in Section 4.3. Finally, the results are discussed in Section 4.4.

4.1 Conventional FMS

A modern FMS automates a number of in-flight tasks. These tasks can be linked to the 4-dimensional trajectory (4D) of the flight. The first dimension in 4D can be interpreted to be linked to the navigation of the aircraft. With the available navigational sources (e.g. satellite and ground based beacons, inertial reference systems and altitude measurement systems) the navigation function of the FMS can estimate the current location, altitude and heading of the aircraft.

The second dimension is related to the in-flight management of the flight plan, where the aircraft is routed along a 2-dimensional route. The FMS sends heading commands to the autopilot in what is called the lateral navigational mode (LNAV) to keep the aircraft on the planned route.

The third dimension is related to the altitude, and there the FMS also takes the altitude information of the flight plan into account to determine the optimal or planned altitude, and commands the autopilot accordingly to maintain or change the altitude along the route. This is called the vertical navigation mode (VNAV). The FMS can also suggest, based on the performance data of the aircraft, an altitude that will give the aircraft better performance for a given Cost Index (CI). The CI indicates the value the airline gives to time in relation to the cost of fuel. The CI has also a relationship with the fourth dimension, the factor time. Time is influenced by the ground speed.

In practice the speed modes available in the FMS determine what airspeed is chosen and how time develops along the flight path. Standard speed modes include 1. Fixed indicated airspeed (IAS)/Mach-number, 2. Econ Mode, and 3. Required Time of Arrival (RTA) Mode. With the fixed IAS/Mach the aircraft operates at a given altitude with a fixed airspeed. The associated ground speed is dependent on the wind conditions. In Econ Mode the FMS makes use of the provided CI and the (predicted) wind conditions to determine dynamically the optimal air speed. With a CI of zero the aircraft will operate at the minimum fuel speed (the speed at which the aircraft flies the greatest distance for the least amount of fuel), and with a CI set to the maximum value the aircraft will operate at the minimum time speed (the speed at which the aircraft flies the greatest distance in the least amount of time). For a given CI the airspeed may change with changing wind conditions. In RTA mode the FMS is also provided with time constraints (RTAs) for given waypoints. The FMS alters the airspeed to get the aircraft at the next (constrained) waypoint at the given RTA time. The FMS considers the (expected) wind conditions in this.

4.2 FMS Logic for Time Windows

One logic that is not available in a conventional FMS is an extension to the RTA mode, where the FMS uses not just a specific RTA time, but a RTA time window.

TWs indicate the allowed flexibility to planned trajectories. A larger TW will allow for greater deviations from the initial planning, without the FMS having to actively correct for the deviation. If a flight is expected to arrive at a specified waypoint outside of its designated time window, a correcting change to the airspeed will be applied. Applying these corrections, the fuel consumption of the aircraft changes.

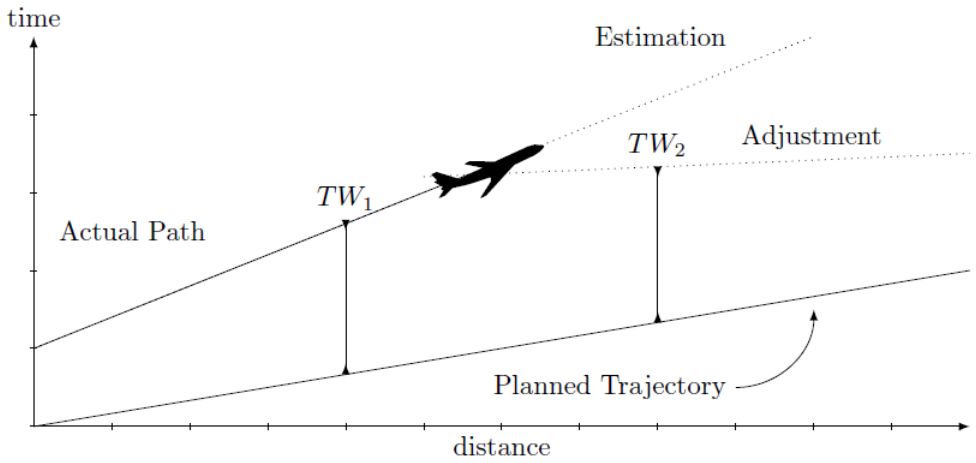

Figure 9 Illustration of the FMS logic.

Figure 9 shows the concept of the FMS logic being applied. The planned trajectory has two sector entries, each with its own time window (TW1, TW2). If a flight deviates from the planned flight, no action needs to be taken as long as the trajectory is projected to be inside the assigned time window. In Figure 9 this can be seen at TW1, the sector is entered at a later time than planned. However, since the entry time is still within the time window no action is needed. For the second sector entry, it can be seen that the predicted flight path will enter the second sector outside the time window. In this case the FMS will apply a velocity change to reach the constrained waypoint within the time window.

In the context of this study a simplified FMS logic for handling time windows is developed.

Whenever the estimated time of arrival (ETA) of a flight, which is already en-route, stays within the required TW, the aircraft operates at its optimal speed. When, however, the flight is expected to operate outside the TW (i.e., ETA outside the TW), the aircraft speed regime is adjusted accordingly at the cost of additional fuel to meet the TWs requirement. To do so, the commanded airspeed of BlueSky is altered accordingly to get the expected arrival time to remain inside the TW. Any initial speed reductions or speed ups are taken into account when determining the updated airspeed. The autopilot logic ensures that the aircraft remains within allowable speed limits.

4.3 Evaluation

To evaluate the effect of the TW approach together with the proposed FMS algorithm, a simulation is performed using the BlueSky ATM simulator [9]. A subset of 5 flight is randomly selected from the solution presented in Section 3. For each flight, the analysis is performed for all 50 ensemble members of the weather data, with a lead time of 24 hrs. This process is repeated for the deterministic TW solution, the probabilistic TW solution and two control scenarios, i.e., the scenario when all flights are required to adhere to TWs of 60 seconds and the scenario when all flights are required to adhere to TWs of 60 minutes, which represent the most and least constraining scenarios.

A number of modification have been made to the BlueSky simulator to facilitate the evaluations of the TWs. Firstly, a module was created that allows the weather data from the ECMWF to be loaded in BlueSky. This module interpolates the weather data and returns the Northward and Eastward component of the wind along the aircraft trajectory. Next, the FMS logic is implemented in BlueSky plugin, as explained in section 4.2. Finally, the trajectory information from the DDR2 database is converted to scenario file (*.scn file). The input file adds the TW constrains on all waypoints along the track. Furthermore, the length of the TWs for a specific flight is the same along all sector entries.

4.4 Results

Table 6 shows preliminary results for the simulation results for 5 flights, randomly chosen the strategic, deterministic TW and stochastic TW solutions presented in Section 3. The type of aircraft is also given. The simulation takes into account 50 weather ensembles, each having associated an equal probability of occuring 1/50. For each flight, the expected fuel consumption (kg) and expected flight time (h:m:s) are presented for the deterministic TW solution and the stochastic TW solution.

Table 6. Evaluation of TWs using BlueSky simulator

Aircraft type	Origin	Destination	Deterministic Model Fuel (kg)	Time h:m:s	TW min	Stochastic Model Fuel (kg)	Time h:m:s	TW min
B739	UKLL	UKBB	1,534	0:33:38	5	1,534	0:33:38	15
A320	LICC	LIRP	2,569	1:01:26	10	2,569	1:01:26	15
B733	EGNM	LPMA	7,583	3:22:41	15	7,583	3:22:41	15
A321	EDDC	LTAI	6,855	2:23:54	15	6,855	2:23:54	15
B738	LTCJ	LTFJ	3,343	1:20:59	15	3,343	1:20:59	15

Table 6 shows that for the set of flights considered, the TWs length is not restrictive when evaluating the expected fuel consumption and the expected flight time. This can be explained by the fact that the variability in the weather ensembles is limited and does not trigger the FMS to enforce large speed changes, and, thus, the changes in the expected fuel consumption are limited. Next steps are to increase the number of flights simulated and consider weather ensembles with larger variability, which is the case for weather forecasts with a lead time of more than 24 hours. The WP3 will provide the results for both the solution scenario (ADAPT solution applied) and the baseline scenario (no ADAPT solution, and thus no TWs) that we will input into our tactical assessment simulations. Furthermore, we have foreseen to apply the following tactical assessment scenarios (as specified in D2.1 Support to medelling activities [12]): inclusion of the wind forecast ensembles from EWCMF into the TWs optimisation model at the tactical level, evaluation of the impact of departure delays on the TWs, and evaluation of the impact of both weather (wind ensembles) and departure delay on the TWs. Also, we will consider the case of extremely limited time windows, e.g., all aircraft having 1 min TW. We will compare the results of these base TW scenarios with the case of deterministic and stochastic TWs.

5 Conclusions and next steps

This delivarables presents a stochastic model that assigns time windows (TWs) to flights taking into account en-route capacity constraints and generic, probabilistic trajectory times. The length of the time windows is an indication of the flexibility assigned to a flight. The results show that, compared to a deterministic time window model, the time windows can be often extended up to 15 min from the optimal times of reaching specific coordinates. The deterministic and stochastic TW models are the input of a flight simulation that assesses the impact of TWs on fuel consumption and flight time.

Next steps are to extend the evaluation of the ADAPT solutions, i.e., the time windows associated with each flight, by means of extensive simulations. The aim of the simulations is to assess the impact of the length of the TWs on the flight time and the fuel consumption needed to adhere to the required TWs. Furthermore, the effects of larger uncertainty factors on the performance of the flights to adhere to the TWs will be evaluated. These include weather ensembles with larger variability, which is the case for weather forecasts with lead times of more than 24 hours and departure time uncertainties, derived from historical flight data.

6 References

[1] Lorenzo Castelli, Luca Corolli, and Guglielmo Lulli. *Critical flights detected with time windows*. Transportation Research Record: Journal of the Transportation Research Board, (2214):103–110, 2011.

[2] Andrew Cook and Damian Rivas. *Complexity science in air traffic management*. Routledge, 2016.

[3] ECMWF. *Description - tigge - ecmwf*, 2018. URL https://software.ecmwf.int/wiki/display/TIGGE/Description.

[4] *User manual for the base of aircraft data (BADA)*. Eurocontrol, 3.6 edition, July 2004.

[5] Eurocontrol. *CODA Digest - all-causes delay and cancellations to air transport in europe*. 2017.

[6] Eurocontrol. *Planning for delay: influence of flight scheduling on airline punctuality*. 2017.

[7] *DDR2 Reference Manual For General Users*. Eurocontrol, 2.9.5 edition, April 2018.

[8] Renate Hagedorn, Roberto Buizza, Thomas M Hamill, Martin Leutbecher, and TN Palmer. *Comparing tigge multimodel forecasts with reforecast-calibrated ecmwf ensemble forecasts*. Quarterly Journal of the Royal Meteorological Society, 138(668):1814–1827, 2012.

[9] Jacco M Hoekstra and Joost Ellerbroek. *Bluesky atc simulator project: an open data and open source approach*. In Proceedings of the 7th International Conference on Research in Air Transportation, pages 1–8. FAA/Eurocontrol USA/Europe, 2016.

[10] Casado, Enrique and La Civita, Marco and Vilaplana, Miguel and McGookin, Euan W, Quantification of aircraft trajectory prediction uncertainty using polynomial chaos expansions, IEEE/AIAA 36th Digital Avionics Systems Conference (DASC), 2017.

[11] Roberson, B. and Pilot, S.S., 2007. Fuel Conservation Strategies: cost index explained. Boeing Aero Quarterly, 2(2007), pp.26-28.

[12] ADAPT Consortium. D2.1 Support to modelling activities, 2018.

7 Acronyms

Acronym	Description
ADP	ATFCM Daily Plan
ANSP	Air Navigation Service Provider
AOBT	Actual Off-Block Time
ASM	Airspace Management
ATC	Air Traffic Control
ATFCM	Air Traffic Flow and Capacity Management
ATM	Air Traffic Management
ATO	Actual Time Over
ATOA	Actual Time Of Arrival
ATOT	Actual Take-Off Time
AU	Airspace User
BADA	Base of Aircraft Data
CDF	Cumulative Density Function
CDM	Collaborative Decision Making
CODA	Central Office for Delay Analysis
CTOT	Calculated Take-Off Time
DDR2	Data Demand Repository
DSLT	Departure Slot Allocation

ECMWF	European Centre for Medium-Range Weather Forecasts
EFPL	Extended Flight Plan
EOBT	Estimated Off-Block Time
ETO	Estimated Time Over
EXOT	Estimated Taxi-Out Time
FMS	Flight Management System
FPL	Flight Plan
GUI	Graphical User Interface
ICAO	International Civil Aviation Organization
IFPS	Integrated Initial Flight Plan Processing System
LNAV	Lateral Navigation Mode of FMS
NMOC	Network Manager Operations Center
NOP	Network Operations Plan
NWP	Numerical Weather Prediction
PDF	Probability Density Function
PMF	Probability Mass Function
RTA	Requested Time of Arrival
SAM	Slot Allocation Message
STOA	Scheduled Time of Arrival
STOT	Scheduled Take-Off Time
TAS	True Air Speed
TW	Time Window
VNAV	Vertical Navigation Mode of FMS
WP	Work Package

-END OF DOCUMENT-